processes

MDPI

Article

Understanding the Lack of Reactivity of 2,4-Dihydroxybenzaldehyde Towards the Biginelli Adduct Using Density Functional Theory Molecular Modeling

Virginia Flores-Morales [1,*], Eduardo D. Ayala-Medrano [1], José García-Elías [1], Margarita L. Martínez-Fierro [2], Edgar Marquez [3,*] and José Mora [4]

1 Laboratorio de Síntesis Asimétrica y Bioenergética (LSAyB), Ingeniería Química (UACQ), Program of Doctorate in Sciences with orientation in Molecular Medicine, Academic Unit of Human Medicine and Health Sciences, Universidad Autónoma de Zacatecas, Campus XXI Km 6 Carr. Zac-Gdl Edificio 6, 98160 Zacatecas, Mexico

2 Laboratorio de Medicina Molecular, Program of Doctorate in Sciences with orientation in Molecular Medicine, Academic Unit of Human Medicine and Health Sciences. Universidad Autónoma de Zacatecas, Campus XXI Km 6 Carr. Zac-Gdl Edificio L1, 98160 Zacatecas, Mexico

3 Grupo de Investigación en Química y Biología, Departamento de Química y Biología, Universidad del Norte, Km 5 vía Puerto Colombia 1569, 081007 Barranquilla Atlántico, Colombia

4 Grupo de Química Computacional y Teórica (QCT-USFQ) and Instituto de Simulación Computacional (ISC-USFQ), Colegio Politécnico de Ciencias e Ingeniería, Universidad San Francisco de Quito, Diego de Robles y Vía Interoceánica, 17-1200841 Quito, Ecuador

* Correspondence: virginia.flores@uaz.edu.mx (V.F.-M.); ebrazon@uninorte.edu.co (E.M.); Tel.: +52-492-116-0699 (V.F.-M.); +57-316-318-2942 (E.M.)

Received: 27 June 2019; Accepted: 24 July 2019; Published: 7 August 2019



Abstract: The Biginelli reaction is a multicomponent reaction for obtaining dihydropyrimidinthiones quickly, with multiple substitution patterns. The reaction mechanism remains unclear. Three possible pathways proposed for the reaction are the iminium route, an enamine intermediate, and the Knoevenagel pathway. However, when thiourea was used, no theoretical calculations were reported. Thus, based on the literature, the iminium pathway was used to obtain evidence explaining the lack of reactivity of 2,4-dihydroxybenzaldehyde towards the Biginelli adduct, compared with 4-hydroxybenzaldehyde. This computational study, carried out using the B3LYP/6-31++G(d,p) level of theory, showed an increment of 150 kJ/mol in the activation energy of the slowest pathway, due to the presence of a hydroxyl group in position 2 (ortho) of the aromatic aldehyde, decreasing its reactivity. Natural bond orbital (NBO) calculations suggest that the determinant steps are simultaneous, i.e., the polarization of the carbonyl group and its corresponding protonation by the hydrogen of the SH fragment of the thiourea tautomer. The activation enthalpy values suggest that the nucleophile attack takes place later on the compound 2,4-dihydroxybenzaldehyde compared to 4-hydroxybenzaldehyde-TS, confirming that the OH group in position 2 hinders the condensation reaction.

Keywords: one-pot reaction; dihydropyrimidinthione derivatives; mechanism reaction; density functional theory; intermediaries

1. Introduction

Also known as Biginelli adducts, 3,4-Dihydropyrimidinones (DHPMs), are compounds derived from pyrimidine, in which carbon C-4 is entirely saturated, eliminating the characteristic aromaticity of

a pyrimidine; a double bond is formed on the C-5 and a second one towards a heteroatom, on carbon C-2. The synthesis of DHPMs (dihydropyrimidines) has become a line of research due to the importance of the antihypertensive [1,2], antibacterial [3,4], antifungal [5,6], antiviral [7], anti-inflammatory, and antineoplastic activity [8,9] they show, through various mechanisms such as calcium channels, GABA agonists, and α1A-adrenergic antagonists [10,11]. Such derivatives can quickly be obtained through the Biginelli reaction, developed in 1893 by Pietro Biginelli [12].

Biginelli´s reaction consists of a one-pot multicomponent reaction between an aldehyde, an active methylene compound, and urea/thiourea or its derivatives [13]. Therefore, the synthesis of DHPMs has become a point of interest of organic synthesis and medicinal chemistry, because this moiety is found in various compounds originating from natural products. The Biginelli reaction gained interest after the 1980s, as it is considered a fundamental reaction in the synthesis of heterocycles and the most common method of obtaining DHPMs and their corresponding dihydropyrimidinones (DHPMs). The synthetic strategy used to obtain these type of nucleus, DHPMs or DHPMTs is broad and varied. The diversity of products, the nature of the reactants and catalyst, the simplicity of reaction systems, and the flexibility of the method make this reaction the best way of obtaining DHPMs and DHPMTs, not to mention better results using microwaves, ultrasound, solvents, and solvent-free conditions.

Even today, the reaction mechanism remains unsolved. Different pathways have been proposed, from acidic conditions in 1933 [14], by Knoevenagel with carbenium ion production in 1973 [15], and contributions made in 1997 by Kappe et al. [16] and in 2009 by De Souza et al. [17] through the density functional theory (DFT) and mass spectroscopy. Other studies using computational chemistry have been presented by Ramos et al. [18] and Puripat et al. [19]. However, there are still doubts regarding substitution patterns not explored for the Biginelli path in obtaining DHPMTs. In this context, one of the compounds obtained by the Biginelli reaction is monastrol, a DHPM with a simple structure designed by Mayer [20].

Monastrol shows antitumor properties by reversibly inhibiting the kinesin-like protein KIF11 (known as Eg5) responsible for the formation and maintenance of the bipolar spindle in mitotic cells. Nevertheless, its weak antimitotic activity and neurotoxicity make it a valuable molecule for the development of antitumor agents, rather than a drug candidate. Therefore, obtaining five DHPMTs from hydroxylated aldehydes, methyl 3-oxobutanoate, and thiourea was crucial in evaluating their synthesis under solvent-free microwave conditions. Under these conditions, it was possible to obtain four Biginelli adducts; however, using 2,4-dihydroxybenzaldehyde, the derivative was not obtained, even after modifying reaction conditions. These results led us to carry out theoretical study in order to understand the unreactivity towards the formation of the Biginelli adduct.

2. Materials and Methods

2.1. Chemistry

The preparation of 1–5 DHPMT derivatives was carried out in a CEM Discovery BenchMate. Melting points were determined on a Fisher-Johns apparatus and are reported uncorrected. The 1H and 13C nuclear magnetic resonance (NMR) spectra were recorded on a JEOL ECA 500 spectrometer equipped with a 5 mm inverse detection pulse field gradient probe at 25 °C at 500 MHz for 1H and 125 MHz for 13C. Chemical shifts are given in values of ppm and referenced to tetramethylsilane (TMS) as an internal standard. Data were measured using a JEOL JMS-T100LC system with low-resolution ionization using direct analysis in real-time mass spectrometry (DART). The spectra of NMR and DART mass spectroscopy are shown in Supplementary Materials. Reactions were monitored by thin-layer chromatography (TLC) on silica gel 60 F254 (Merck, Ciudad de Mexico, Mexico)

2.2. Synthesis of DHPMT Derivatives

Analytical grade benzaldehyde, salicylaldehyde, 3-hydroxybenzaldehyde, 4-hydroxybenzaldehyde, 2,4-dihydroxybenzaldehyde, methyl acetoacetate (MAA), and thiourea were purchased from

Sigma-Aldrich Co. (Ciudad de Mexico, Mexico). Commercially available solvents (acetone, chloroform, and methanol) were used after purification; then, the products were dried according to standard procedures. In a flask fitted with a stirring system, the corresponding aldehyde (1.0 equiv.) was placed together with 3-oxobutanoic acid methyl ester (1.1 equiv.) and thiourea (1.1 equiv.). All products were obtained under microwave-assisted reactions on a CEM Discovery BechMate system with 100 W potency, and the temperature was 100 °C for each reaction in an open-vessel system. The reaction time was determined for each adduct by TLC. Each adduct was monitored every 5 min; the end of the reaction was established once the starting material was consumed and a total reaction yield was calculated. The solid product was vacuum filtered and washed with solvent.

2.3. Characterization of Compounds

Characterization of the compounds ^{1}H NMR, ^{13}C NMR, and DART MS was carried out using their melting point (mp), as follows (see Figure 1):

(1) *4-phenyl-6-methyl-5-methoxycarbonyl-3,4-dihydropyrimidyn-2(H)-thione (DHPMT 01)*. White solid; mp 224–226 °C [Lit. 228–229] [21]. Yield: 57% (70 mg); acetone soluble. ^{1}H-NMR ($CDCl_3$, 500 MHz): δ(ppm) = 9.25 (H-1, sa, 1H), 8.67 (H-3, sa, 1H), 7.31 (H-9-11, m, 3H), 7.25 (H-8 & 12, m, 2H), 5.40 (H-4, d, J = 3.7 Hz, 1H), 3.60 (H-15, s, 3H), 2.40 (H-16, s, 3H). ^{13}C-NMR ($CDCl_3$,125 MHz): δ(ppm) = 176.5 (C-2), 166.6 (C-13), 145.5 (C-6), 144.5 (C-7), 129.5 (C-8, C-12), 128.7 (C-10), 127.5 (C-9, C-11), 102.6 (C-5), 56.0 (C-15), 51.4 (C-4), 17.9 (C-16). DART MS m/z 263 [M+1] (calculated for $C_{13}H_{14}N_2O_2S$, 262.3275).

(2) *4-(2-hydroxyphenyl)-6-methyl-5-methoxycarbonyl-3,4-dihydropyrimidyn-2(H)-thione (DHPMT 02)*. White powder; mp 206–209 °C [Lit. 209–212] [22] Yield 25% (30 mg); methanol soluble. ^{1}H-NMR (CD_3OD, 500 MHz): δ(ppm) = 7.22 (H-10, td, J = 8.1, 1.7 Hz, 1H), 7.21 (H-12, ddd, J = 7.2, 1.7, 0.8 Hz; 1H), 6.94 (H-11, td, J = 7.45, 1.0 Hz, 1H), 6.83 (H-9, dt, J = 8.1, 0.5 Hz, 1H) 4.74 (H-4, d, J = 2.6 Hz, 1H), 3.78 (H-15, s, 3H), 1.87 (H-16, s, 3H). ^{13}C-NMR (CD_3OD, 125 MHz): δ(ppm) = 185.5 (C-2), 178.3 (C-13), 168.6 (C-8), 152.1 (C-6), 131.1 (C-10) 129.6 (C-12), 124.3 (C-7), 122.5 (C-11), 117.9 (C-9), 82.6 (C-5), 52.8 (C-15), 44.2 (C-4), 24.0 (C-16). DART MS m/z 279 [M+1] (calculated for $C_{13}H_{14}N_2O_3S$, 278.3268).

(3) *4-(3-hydroxyphenyl)-6-methyl-5-methoxycarbonyl-3,4-dihydropyrimidyn-2(H)-thione (DHPMT 03)*. White powder; mp 222–224 °C [Lit. 220–222] [23]. Yield 25% (30 mg); methanol soluble. ^{1}H-NMR (CD_3OD, 500 MHz): δ(ppm) = 10.34 (H-1, d, J = 1.9 Hz, 1H), 9.64 (H-3, dd, J = 3.9, 1.9 Hz, 1H) 9.47 (H-18, s, 1H), 7.12 (H-11, t, J = 7.7 Hz, 1H), 6.70-6.60 (H-8,10&12, m, 3H), 5.09 (H-4, d, J = 3.9 Hz, 1H), 3.56 (H-15, s, 3H), 2.28 (H-16, s, 3H). ^{13}C-NMR (CD_3OD, 125 MHz): δ(ppm) = 174.2 (C-2), 165.7 (C-13), 157.5 (C-9), 145.2 (C-6), 144.7 (C-4), 129.7 (C-11), 117.0 (C-12), 113.2 (C-10), 100.5 (C-5), 53.8 (C-15), 51.2 (C-4), 17.3 (C-16).

(4) *4-(4-hydroxyphenyl)-6-methyl-5-methoxycarbonyl-3,4-dihydropyrimidyn-2(H)-thione (DHPMT 04)*. White powder; mp 258–260 °C [Lit. 246-248] [24]; Yield 31% (70 mg); methanol soluble. ^{1}H-NMR (CD_3OD, 500 MHz): δ(ppm) = 7.09 (H-8&12, ddd, J = 8.7, 3.0, 2.0 Hz, 2H), 6.72 (H-9&11, ddd, J = 8.7, 3.0, 2.0 Hz, 2H), 5.21 (H-4, s, 1H), 3.62 (H-15, s, 3H), 2.34 (H-16, s, 3H). ^{13}C-NMR (CD_3OD, 125 MHz): δ(ppm) = 176.0 (C-2), 167.9 (C-13), 158.4 (C-10), 145.5 (C-6), 129.0 (C-8, C-12) 116.3 (C-9, C-11), 103.3 (C-5), 55.9 (C-15), 51.7 (C-4), 17.6 (C-16). DART MS m/z 279 [M+1] (calculated for $C_{13}H_{14}N_2O_3S$, 278.3268).

(5) *4-(2,4-dihydroxyphenyl)-6-methyl-5-methoxycarbonyl-3,4-dihydropyrimidyn-2(H)-thione (DHPMT 05)*. 2,4-dihydroxybenzaldehyde 50 mg (0.36 mmol), 0.04 mL (50 mg, 0.39 mmol) of MAA, 30 mg (0.39 mmol) of thiourea and p-toluenesulfonic acid catalytic, 15–60 min reaction. The Biginelli adduct was not obtained.

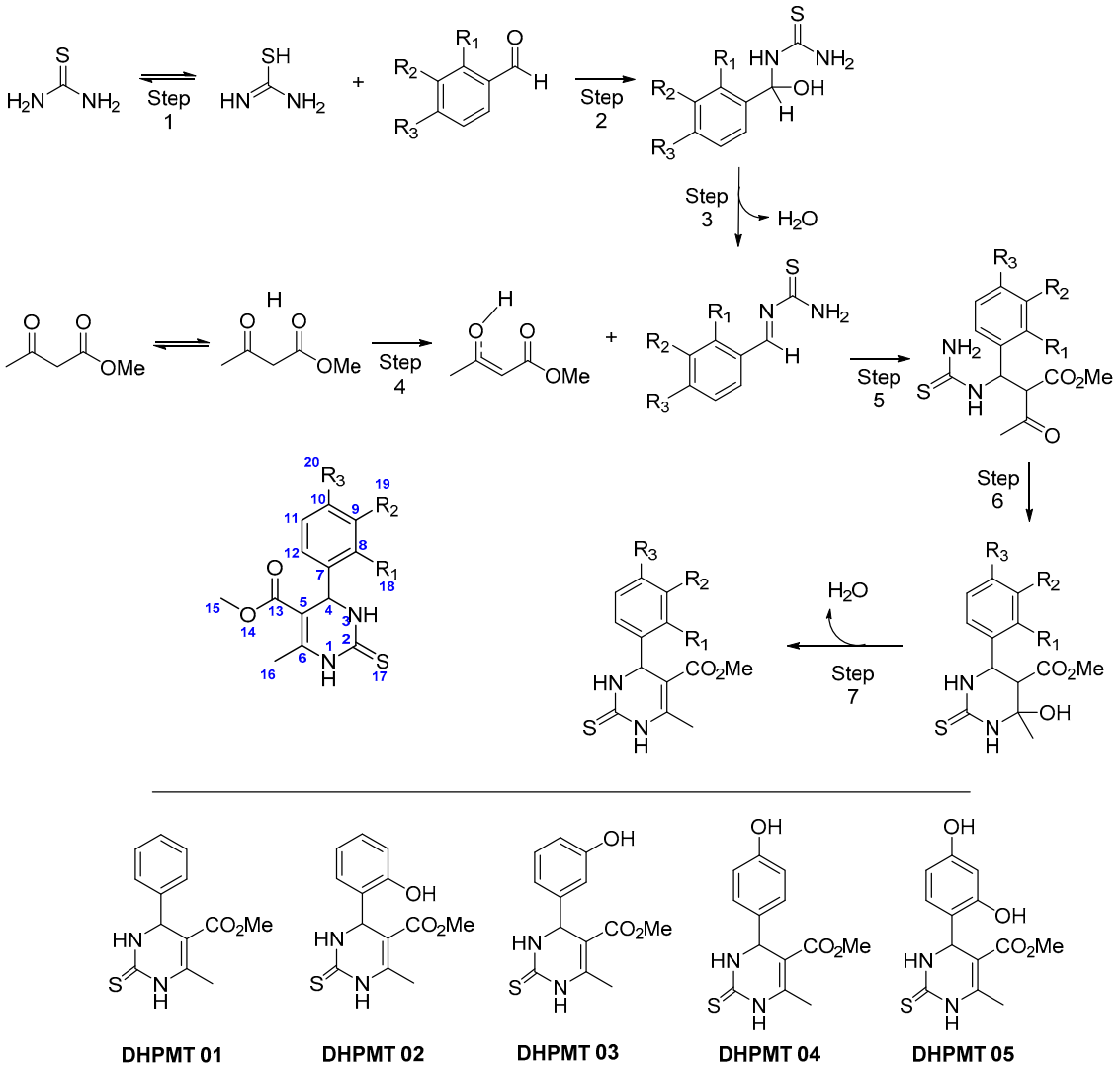


Figure 1. Biginelli pathway reaction for selected aromatic aldehyde, according to iminium route.

2.4. Theoretical Methods and Molecular Modeling

The potential energy surface (PES) of all species involved in the reactions of 4-hydroxybenzaldehyde and 2,4-dihydroxybenzaldehyde with MAA and thiourea was studied employing DFT and transition state theory (TST). The interchange-correlation functional of Becke, Lee, Yang, and Parr, jointly basis set 6-31++G(2d,p), was employed by the use of Gaussian 09 for Linux [25]. Because the reactions were carried out free of solvents, they were modelled in the vacuum. The minimum energy surface (MES) was generated using the following convergence criterion: maximum displacement 0.0018 Å and maximum force: 0.00045 Hartree/Bohr. Three mechanisms were studied, iminium route, enamine intermediate route, and Knoevenagel pathway without solvent; however, only the mechanism with the lowest activation energy was analyzed herein.

The stationary points, minimum energy structure, and saddle point were verified employing frequency calculations, using statistical mechanics. Additionally, unimolecular and bimolecular transition states were obtained using the quadratic synchronous transit method (QST) with two (QST2) or three (QST3) structures. The calculation of intrinsic reaction coordinates (IRC) in all cases confirmed these structures. This method allowed the verification of first-order nature; it means that the reactant or reactants connect to products through a simple reaction coordinate. Thermodynamic magnitudes, such as zero-point energy (ZPE), absolutes entropies, S(T) enthalpy, and H(T), were obtained from quantum mechanics and statistic mechanics, using partition functions. The velocity coefficient, activation

energy (Ea), activation enthalpy (ΔH‡), and Gibbs energy (ΔG‡) were calculated from transition state theory (TST) assuming the transmission coefficient to be equal to 1, using equations previously described [26–28].

2.4.1. Transition State and Mechanism

Even when Biginelli reactions are one of the most used reactions in organic synthetic literature, the reaction mechanism remains unclear. Several attempts have been made to elucidate the mechanism. In this sense, three possible pathways proposed for the reaction of aromatic aldehyde, urea, and methyl acetoacetate: Iminium route, enamine-intermediate, and Knoevanagel pathway (Figure 2) [13]. Some works have reported theoretical calculations that supplied sharp pieces of evidence that the iminium route is likely to occur when urea used as reagent [17,18,29,30]. However, no theoretical calculations had reported when thiourea was used. Thus, based on literature, the three pathway described above were studied to get some evidence that explained the unreactivity of 2,4-dihydroxybenzaldehyde to Biginelli adduct. Also, only the mechanism with the lowest activation energy was analyzed herein. The kinetic mechanism of iminium route studied for both compounds because of the structural similarity between 4-hydroxybenzaldehyde, 2,4-dihydroxybenzaldehyde. Figure 1 shows the reactions involved in the selected compounds. According to literature, the first step (1) in the iminium route is the nucleophilic addition of thiourea to aromatic aldehyde, followed by dehydration of the adduct formed in step 1; this compound (3) reacts with MAA to yield the 5 compounds, which produces a six-member ring and dehydrated to form the Biginelli adducts.

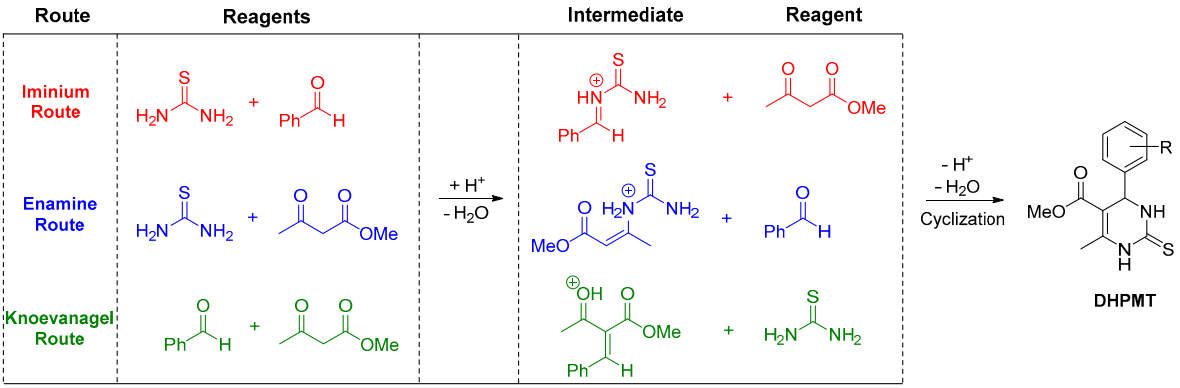


Figure 2. Biginelli pathway reaction: Iminium route, enamine intermediate, and Knoevanagel pathway.

2.4.2. Bond Order Analysis

The process of bond rupture and formation in the transition state for the slowest stage of the reaction in the iminium pathway was studied employing natural bond orbitals (NBOs) where Wiberg bond indexes were calculated using the NBO 5.0 program, which operates within the Gaussian 09W software package [31]. These parameters allow the yield of the relative change rate of the bond and the development percentage (%) of each bond, which indicates whether the coordinate is "early" or "late" in the slowest step (Equation (1)). It can be noted that these calculations were made only for the slowest stages in both cases.

$$\%E_v = \delta B_i * 100, \quad (1)$$

where δBi is the relative variation of the bond index and defined by Equation (2):

$$\frac{\left[B_i^{TS} - B_i^R\right]}{\left[B_i^p - B_i^R\right]}, \quad (2)$$

The superscripts ^{R}, ^{TS}, and ^{P} represent the reactant, transition state, and products, respectively. The synchronicity parameter is used to explain whether a concerted reaction proceeds synchronously, where all events have the same progress along the reaction coordinate (Sy = 1), or whether the reaction is entirely asynchronous (Sy = 0) (Equation (3)).

$$S_y = 1 - \frac{\left[\sum_{i=1}^{n} \frac{|\delta B_i - \delta B_{av}|}{\delta B_{av}}\right]}{2n-2}. \quad (3)$$

3. Results and Discussion

3.1. Chemistry

The methodology was used from the procedures reported by Stadler and Kappe [32] and Manhas et al. [33], with an environmentally friendly approach using microwave conditions, a solvent-free system, and low-cost acid catalyst [30]. The results are shown in Table 1.

Table 1. Results of the synthesis of DHPMTs derivatives.

Entry	Compounds	Time (min)	Yield (%)	mp (°C)	Solubility
1	DHPMT 01	25	57	224–226	Acetone
2	DHPMT 02	5	25	206–209	Methanol
3	DHPMT 03	5	25	222–224	Methanol
4	DHPMT 04	10	31	258–260	Methanol
5	DHPMT 05	15–60	–	–	–

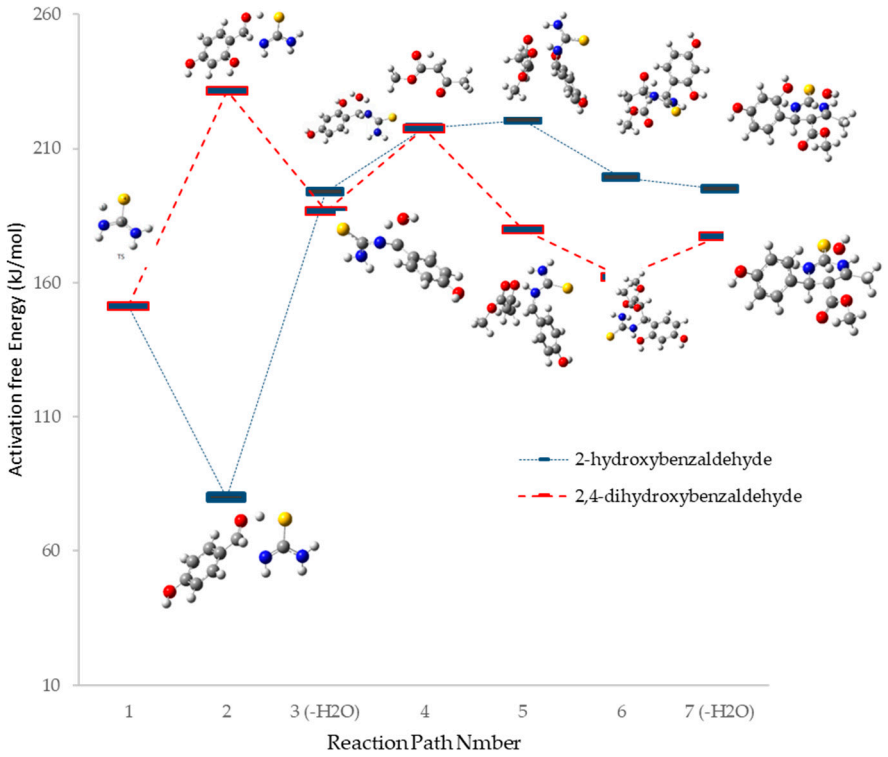
In order to obtain DHPMT 05, various catalysts were evaluated such as $FeCl_3$ $6H_2O$, $TiCl_4$, HCl, $ZnCl_2$, and piperazine, according to Wan et al. [34]. None of the Lewis acids used in previous syntheses favored exclusively some of the reactions that developed, and presented different behaviors among them, although they presented the same by-products. The use of piperazine as a catalyst leading to the acquisition of a solid-phase product with a yield of 72% with a reaction time of 15 minutes. The spectroscopic analysis showed the presence of dienamine produced by the condensation between piperazine and methyl acetoacetate. This result led us to explore the reaction mechanism using theoretical methods (DFT) and molecular modeling.

3.2. Thermodynamic Parameters for 4-Hydroxybenzaldehyde and 2,4-Dihydroxybenzaldehyde

Table 2 shows the kinetic and thermodynamic activation parameters obtained at B3LYP/6-31++G(2d,p) for all reaction pathways in the iminium route; Scheme 1 reveals the free energy profile for each TS along with the reaction pathway. The reaction was studied in six (6) steps as follows: The first step corresponds to the condensation reaction between thiourea and the benzaldehyde. In this step, it was found that the tautomerization of thiourea had an equilibrium constant in the order of 10^{-2}; therefore, there is a significant population of thiol tautomer. Step 2 corresponds to the reaction of the thiol tautomer of the previous step with the benzaldehyde through six-member TS. Step 3 corresponds to the elimination of water from the product obtained in the second step. Step 4 corresponds to the keto-enol tautomerization reaction of MAA; this enol reacts in step five with the compound originated in step 3; subsequently, the compound generated in step 5 reacts through an intramolecular mechanism generating a cyclic compound (step 6) which finally lost a water molecule forming the DHPMT compound (1–5).

Table 2. Kinetic and thermodynamic activation energies obtained in each stage of the Biginelli reaction, studied at the B3LYP/6-31++G(2d,p) level of theory for 4-hydroxybenzaldehyde and 2,4-dihydroxybenzaldehyde.

Step	ΔH ≠ kJ/mol	EA kJ/mol	ΔG ≠ kJ/mol	ΔS ≠ kJ/mol
4-hydroxybenzaldehyde				
1	150.83	153.31	151.21	−1.28
2	27.96	30.44	79.88	−172.92
3 (−H2O)	195.62	198.09	193.57	6.89
4	212.77	215.25	217.49	−14.37
5	169.65	172.13	220.55	−170.70
6	183.97	186.44	199.01	−50.46
7 (−H2O)	195.92	198.40	194.68	4.17
2,4-dihydroxybenzaldehyde				
1	150.83	153.31	151.2103	−1.28
2	283.19	285.67	231.51	−173.33
3 (−H2O)	191.23	193.71	186.56	15.67
4	212.77	215.25	217.49	−14.372
5	121.13	123.61	179.94	−47.14
6	151.57	154.05	162.28	−36.16



Scheme 1. Reaction energy diagram for Biginelli adduct's formation from 2-Hydroxybenzaldehide and 2,4-dihidroxybenzaldehide at B3LYP/6-31++G(2d,p).

According to Scheme 1, there is an evident difference in the activation free energy of stage 2 observed for each compound. This stage is faster for the 4-hydroxybenzaldehyde compound than for 2,4-dihydroxybenzaldehyde. The high free energy value for this last compound (approximately 239 kJ/mol) means that, in practice, the condensed product was not obtained; therefore, as it is a determining stage compared to other stages, it prevents the formation of the final product. According to the structural similarity of these compounds, the results suggest that the presence of the OH group in the ortho position of the aldehyde hinders the introduction of thiourea for condensation to take

place. The rest of the stages are more feasible for both compounds, with relatively low activation free energy in each case.

3.3. Reaction Mechanism and Geometric Parameters

Figure 3 shows the structures of minimum energies for R, TS, and P for each case studied. The condensation reaction with thiourea occurs through a six-member cyclic transition state, of a concerted nature, unlike what is reported in the literature for the case of urea as the reagent, where it is considered that the reaction occurs in several stages. Within the level of theory used herein, it was found that the TS of six members is approximately 70 kcal/mol lower than the corresponding TS of 4 members.

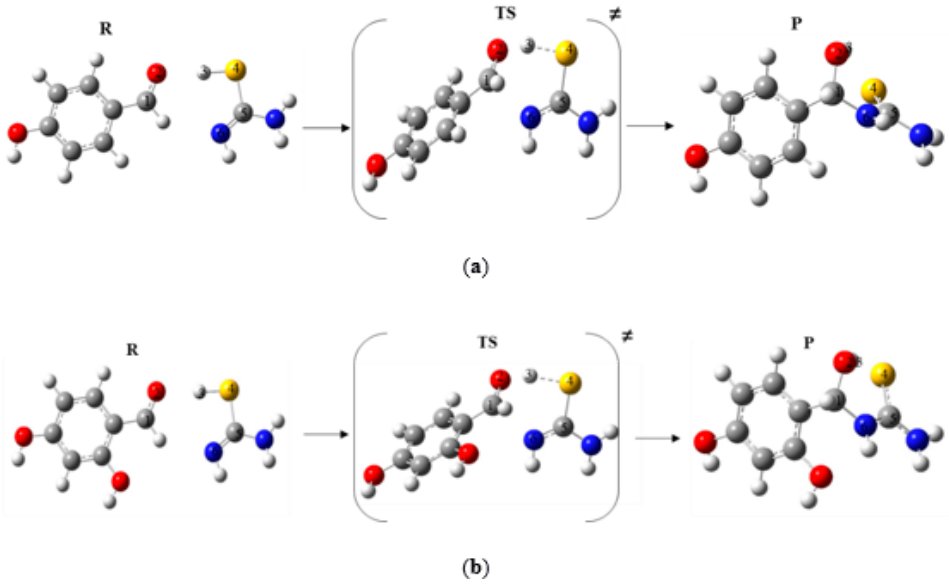


Figure 3. Minimum energy structures for reactant (R), transition state (TS), and products (P), for the second stage of the Biginelli reaction studied at the B3LYP/6-31++G(2d,p) level of theory. (**a**) 4-hydroxybenzaldehyde; (**b**) 2,4-dihydroxybenzaldehyde.

Geometric parameters such as bond length, dihedral angles, and imaginary frequency associated with the transition vector in the TS are shown in Tables 3 and 4. In both cases, there is an increase in the distance of bonds C10–O11 and H21–S22, and a decrease in interatomic distances for bonds O11–H21 and N15–C1O. These results suggest that this reaction stage is carried out through polar-TS, where the hydrogen HS protonates to the carbonyl group of the benzaldehyde, which is polarized later to be attacked by the NH atom of the thiourea compound through a concerted process. The values of the dihedral angles in both cases suggest transition states far from planarity.

Table 3. Structural parameters for R, TS, and P, involved in the Biginelli reaction, from the B3LYP/6-31++G(2d,p) level of theory for 4-hydroxybenzaldehyde.

Structure	C1–O2	O2–H3	H3–S4	S4–C5	C5–N6	N6–C1
R	1.222	1.997	1.357	1.785	1.279	3.421
TS	1.285	1.242	1.605	1.761	1.297	2.162
P	1.402	0.976	2.389	1.678	1.360	1.360
Angle	C1-O2-H3-S4	02-H3-S4-C5	H3-S4-C5-N6	S4-C5-N6-C1	C5-N6-C1-O2	N6-C1-O2-H3
TS	46.982	−2.610	−8.199	3.078	2.785	−46.103
μTS = 5.7215 Debye Imaginary Frequency (cm^{-1}) = 903.39						

Table 4. Structural parameters for R, TS, and P, involved in the Biginelli reaction, from the B3LYP/6-31++G(2d,p) level of theory for 2,4-dihydroxybenzaldehyde.

Structure	C1–O2	O2–H3	H3–S4	S4–C5	C5–N6	N6–C1
R	1.225	1.978	1.359	1.785	1.278	3.420
TS	1.267	1.204	1.644	1.761	1.296	2.230
P	1.430	0.960	1.608	1.780	1.338	1.470
Angle	C1-O2-H3-S4	02-H3-S4-C5	H3-S4-C5-N6	S4-C5-N6-C1	C5-N6-C1-O2	N6-C1-O2-H3
TS	47.157	−2.159	−15.285	−1.518	40.887	−46.005
μTS = 5.5015 Debye Imaginary Frequency (cm^{-1}) = 1003.39						

The distance N6–C1 in TS, which represents the nucleophilic attack on the reaction center for the 2,4-dihydroxybenzaldehyde compound, is more significant for the 4-hydroxybenzaldehyde which provides additional evidence that the OH group at position 2 of the aromatic ring prevents a fundamental approach of the nucleophile to the reaction center. The decrease in the polarity of the TS, when the 4-hydroxybenzaldehyde compares to 2,4-dihydroxybenzaldehyde compound, suggests that the presence of the OH group in position ortho decreases the polarization of the TS and therefore the rate of the reaction.

The influence of the OH group on the reduction of TS polarization is supported by the values of the NBO charges shown in Table 5. The high dispersion of charges can be observed in atoms C11, O12, H22, and S23 from 4-hydroxybenzaldehyde. These results would confirm the hypothesis that the OH group in position 2 in 2,4-dihydroxybenzaldehyde prevents the nucleophile substitution by disadvantaging the polarization of the carbonyl group, the transfer of the proton to this group, and consequently, an increase of activation energy at this stage.

Table 5. Wiberg bond indexes of R, TS, and P, for the Biginelli reaction of 4-hydroxybenzaldehyde and 2,4-dihydroxybenzaldehyde in gas phase obtained from B3LYP/6-31++G(2d,p).

4-hydroxybenzaldehyde							
Bond	**C1–O2**	**O2–O3**	**H3–S4**	**S4–C5**	**C5–N6**	**N6–C1**	**Sy**
R	1.738	0.043	0.906	1.075	1.758	0.001	
TS	1.297	0.417	0.206	1.171	1.569	0.387	
P	0.972	0.773	0.007	1.513	1.196	0.930	0.739
βB_i	0.575	0.593	0.779	0.217	0.336	0.415	
% Ev	44.52	51.25	77.94	21.77	33.63	41.55	
2,4-dihydroxybenzaldehyde							
R	1.730	0.0342	1.075	1.075	1.764	0.0001	
TS	1.393	0.238	0.522	1.173	1.604	0.249	
P	0.996	0.903	0.277	1.305	1.286	0.911	0.963
βB_i	0.459	0.234	0.692	0.426	0.334	0.376	
% Ev	45.91	43.50	69.29	42.61	33.47	37.60	

The Wiberg bond indexes were calculated with the purpose of studying the evolution of the reaction, along with the coordinates involved in product formation. The evolution of the bonds and the order of synchronicity are shown in Table 5 for each studied stage. In both reactions, the determining stages are the polarization of the H3–S4 bond and the protonation of the carbonyl group of the benzaldehyde substituted, respectively. However, the difference in the evolution of these bonds for both compounds is remarkable. In the case of the 4-hydroxybenzaldehyde, the partial formation of the O2–H3, and N6–C1 bonds, as well as the polarization of the C1–O2 bond during the TS is noteworthy. In contrast, the bond order for the 2,4-dihydroxybenzaldehyde compound is much smaller, confirming that the last TS interaction occurs subsequently and, therefore, the condensation reaction is slower.

On the other hand, the synchronicity of the reaction confirms the decrease of the TS polarity in this case and, consequently, a lower reactivity.

The magnitude of the interaction between the respective aromatic compounds and the tautomer of thiourea can be estimated by observing the interactions between orbital boundaries of both compounds. Figure 4 shows the highest occupied molecular orbital (HOMO) for thiourea and the lowest occupied molecular orbital (LUMO) of the substituted benzaldehydes. It can see that the decrease in distance between C10 and N19 implies subsequent interaction among the OH group, with the N atom causing a strong electronic repulsion amid two electronegative groups; this secondary interaction an effective interaction, making the formation of the condensation product difficult.

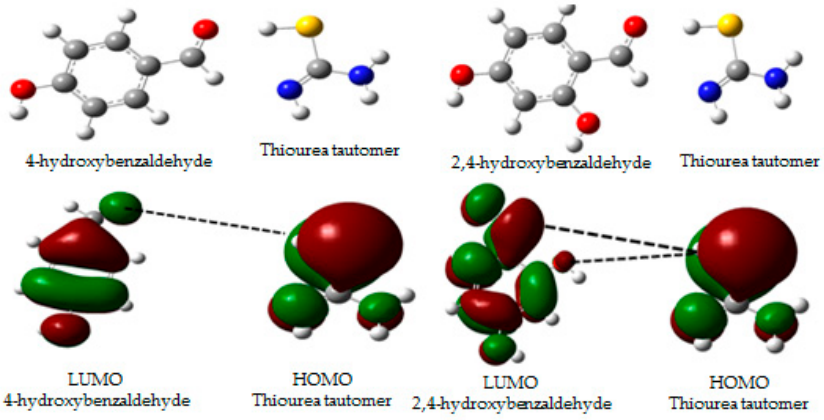


Figure 4. Interactions between the lowest unoccupied molecular orbital (LUMO) of the 4-hydroxybenzaldehyde and 2,4-dihydroxybenzaldehyde compounds and highest occupied molecular orbital (HOMO) of the thiourea tautomer (nucleophile).

4. Conclusions

The methodology used, free of solvents, allowed us to yield derivatives with reaction times lower than those reported in the literature. The non-reactivity of 2,4-dihydroxybenzaldehyde was evaluated experimentally using different catalysts and reaction conditions, without success; thus, to explain the lack of 2,4-dihydroxybenzaldehyde, molecular modeling was necessary. According to the thermodynamic activation parameters, stage 2, which corresponds to the condensation between thiourea (tautomer) and the corresponding aromatic aldehyde, is crucial for determining the reactivity of hydroxylated benzaldehydes towards the Biginelli reaction. The presence of a hydroxyl group in position two at the reaction center (carbonyl group) increases activation energy by approximately 150 kJ/mol; consequently, the reactivity of these compounds decreases. The NBO calculations suggest that the determining pathways are, simultaneously, the polarization of the carbonyl group and its corresponding protonation by hydrogen of the SH fragment of the thiourea tautomer. The results show that the nucleophile attack corresponds to a late transition state for the compound 2,4-dihydroxybenzaldehyde, proving that the OH group in position 2 hinders the condensation reaction.

Supplementary Materials: The following are available online at http://www.mdpi.com/2227-9717/7/8/521/s1.

Author Contributions: Conceptualization, V.F.-M. and E.M.; Methodology, E.D.A.-M., J.G.-E., and J.M.; Software, V.F.-M. and E.M.; Validation, V.F.-M. and J.G.-E.; Formal analysis, V.F.-M., M.L.M.-F., and E.M.; Investigation, V.F.-M. and E.M.; Writing—original draft preparation, V.F.-M. and E.M.; Writing—review and editing, V.F.-M. and E.M.; Project administration, V.F.-M.; Funding acquisition, V.F.-M.

Funding: This work was supported in part by an LSAyB internal grant.

Acknowledgments: Virginia Flores-Morales is grateful to Carlos F. Bautista Capetillo and the PFCE (2016–2017) program of Área de Ingenierías y Tecnológicas for their support to conduct a research stay at the Universidad del Norte.

Conflicts of Interest: The authors declare no conflict of interest.

References

1. Farghaly, A.M.; Aboulwafa, O.M.; Elshaier, Y.A.M.; Badawi, W.A.; Haridy, H.H.; Mubarak, H.A.E. Design, synthesis, and antihypertensive activity of new pyrimidine derivatives endowing new pharmacophores. *Med. Chem. Res.* **2019**, *28*, 360–379. [CrossRef]
2. Chikhale, R.V.; Bhole, R.P.; Khedekar, P.B.; Bhusari, K.P. Synthesis and pharmacological investigation of 3-(substituted 1-phenylethanone)-4-(substituted phenyl)-1, 2, 3, 4-tetrahydropyrimidine-5-carboxylates. *Eur. J. Med. Chem.* **2009**, *44*, 3645–3653. [CrossRef] [PubMed]
3. Sedaghati, B.; Fassihi, A.; Arbabi, S.; Ranjbar, M.; Memarian, H.R.; Saghaie, L.; Omidi, A.; Sardari, A.; Jalali, M.; Abedi, D. Synthesis and antimicrobial activity of novel derivatives of Biginelli pyrimidines. *Med. Chem. Res.* **2012**, *21*, 3973–3983. [CrossRef]
4. Ramachandran, V.; Arumugasamy, K.; Singh, S.K.; Edayadulla, N.; Ramesh, P.; Kamaraj, S.-K. Synthesis, antibacterial studies, and molecular modeling studies of 3,4-dihydropyrimidinone compounds. *J. Chem. Boil.* **2015**, *9*, 31–40. [CrossRef] [PubMed]
5. Wani, M.Y.; Ahmad, A.; Kumar, S.; Sobral, A.J. Flucytosine analogues obtained through Biginelli reaction as efficient combinative antifungal agents. *Microb. Pathog.* **2017**, *105*, 57–62. [CrossRef] [PubMed]
6. Matos, L.H.S.; Masson, F.T.; Simeoni, L.A.; Homem-De-Mello, M. Biological activity of dihydropyrimidinone (DHPM) derivatives: A systematic review. *Eur. J. Med. Chem.* **2018**, *143*, 1779–1789. [CrossRef] [PubMed]
7. Kumarasamy, D.; Roy, B.G.; Rocha-Pereira, J.; Neyts, J.; Nanjappan, S.; Maity, S.; Mookerjee, M.; Naesens, L. Synthesis and in vitro antiviral evaluation of 4-substituted 3,4-dihydropyrimidinones. *Bioorg. Med. Chem. Lett.* **2017**, *27*, 139–142. [CrossRef] [PubMed]
8. Dinakaran, V.S.; Jacob, D.; Mathew, J.E. Synthesis and biological evaluation of novel pyrimidine-2(1H)-ones/thiones as potent anti-inflammatory and anticancer agents. *Med. Chem. Res.* **2012**, *21*, 3598–3606. [CrossRef]
9. Elumalai, K.; Ali, M.A.; Elumalai, M.; Eluri, K.; Srinivasan, S.; Mohanty, S.K. Microwave assisted synthesis of some novel acetazolamide cyclocondensed 1,2,3,4-tetrahydropyrimidines as a potent antimicrobial and cytotoxic agents. *Beni-Suef Univ. J. Basic Appl. Sci.* **2014**, *3*, 24–31. [CrossRef]
10. Kaur, R.; Chaudhary, S.; Kumar, K.; Gupta, M.K.; Rawal, R.K. Recent synthetic and medicinal perspectives of dihydropyrimidinones: A review. *Eur. J. Med. Chem.* **2017**, *132*, 108–134. [CrossRef]
11. De Fátima, Â.; Braga, T.C.; Neto, L.D.S.; Terra, B.S.; Oliveira, B.G.F.; da Silva, D.L.; Modolo, L.V. A mini-review on Biginelli adducts with notable pharmacological properties. *J. Adv. Res.* **2015**, *6*, 363–373. [CrossRef] [PubMed]
12. Tron, G.C.; Minassi, A.; Appendino, G.B. Pietro Biginelli: The Man behind the Reaction. *Eur. J. Org. Chem.* **2011**, *2011*, 5541–5550. [CrossRef]
13. Nagarajaiah, H.; Mukhopadhyay, A.; Moorthy, J.N. Biginelli reaction: An overview. *Tetrahedron Lett.* **2016**, *57*, 5135–5149. [CrossRef]
14. Folkers, K.; Johnson, T.B. Researches on Pyrimidines. CXXXVI. The Mechanism of Formation of Tetrahydropyrimidines by the Biginelli Reaction1. *J. Am. Chem. Soc.* **1933**, *55*, 3784–3791. [CrossRef]
15. Sweet, F.; Fissekis, J.D. Synthesis of 3,4-dihydro-2(1H)-pyrimidinones and the mechanism of the Biginelli reaction. *J. Am. Chem. Soc.* **1973**, *95*, 8741–8749. [CrossRef]
16. Kappe, C.O. A Reexamination of the Mechanism of the Biginelli Dihydropyrimidine Synthesis. Support for anN-Acyliminium Ion Intermediate. *J. Org. Chem.* **1997**, *62*, 7201–7204. [CrossRef]
17. De Souza, R.O.M.A.; Da Penha, E.T.; Milagre, H.M.S.; Garden, S.J.; Esteves, P.M.; Eberlin, M.N.; Antunes, O.A.C. The Three-Component Biginelli Reaction: A Combined Experimental and Theoretical Mechanistic Investigation. *Chem. Eur. J.* **2009**, *15*, 9799–9804. [CrossRef]
18. Ramos, L.M.; Tobio, A.Y.P.D.L.Y.; Dos Santos, M.R.; De Oliveira, H.C.B.; Gomes, A.F.; Gozzo, F.C.; De Oliveira, A.L.; Neto, B.A.D. Mechanistic Studies on Lewis Acid Catalyzed Biginelli Reactions in Ionic Liquids: Evidence for the Reactive Intermediates and the Role of the Reagents. *J. Org. Chem.* **2012**, *77*, 10184–10193. [CrossRef]
19. Puripat, M.; Ramozzi, R.; Hatanaka, M.; Parasuk, W.; Parasuk, V.; Morokuma, K. The Biginelli Reaction Is a Urea-Catalyzed Organocatalytic Multicomponent Reaction. *J. Org. Chem.* **2015**, *80*, 6959–6967. [CrossRef]
20. Mayer, T.U. Small Molecule Inhibitor of Mitotic Spindle Bipolarity Identified in a Phenotype-Based Screen. *Science* **1999**, *286*, 971–974. [CrossRef]

21. Shaabani, A.; Rahmati, A. Ionic liquid promoted efficient synthesis of 3,4-dihydropyrimidin-2-(1H)-ones. *Catal. Lett.* **2005**, *100*, 177–179. [CrossRef]
22. Liu, Q.; Pan, N.; Xu, J.; Zhang, W.; Kong, F. ChemInform Abstract: Microwave-Assisted and Iodine-Catalyzed Synthesis of Dihydropyrimidin-2-thiones via Biginelli Reaction under Solvent-Free Conditions. *Cheminform* **2013**, *43*. [CrossRef]
23. Mukhopadhyay, C.; Datta, A. The development of an ecofriendly procedure for alkaline metal (II) sulfate promoted synthesis of N,N′-dimethyl substituted (unsubstituted)-4-aryl-3,4-dihydropyrimidones (thiones) and corresponding bis-analogues in aqueous medium: Evaluation by green chemistry metrics. *J. Heterocycl. Chem.* **2010**, *47*, 136–146.
24. Ma, J.; Zhong, L.; Peng, X.; Sun, R. d-Xylonic acid: A solvent and an effective biocatalyst for a three-component reaction. *Green Chem.* **2016**, *18*, 1738–1750. [CrossRef]
25. Frisch, M.J.; Trucks, G.W.; Schlegel, H.B.; Scuseria, G.E.; Robb, M.A.; Cheeseman, J.R.; Scalmani, G.; Barone, V.; Petersson, G.A.; Nakatsuji, H.; et al. *Gaussian16 Revision B.01*; Gaussian, Inc.: Wallingford, UK, 2016.
26. Márquez, E.; Domiínguez, R.M.; Mora, J.R.; Coórdova, T.; Chuchani, G. Experimental and Theoretical Studies of the Homogeneous, Unimolecular Gas-Phase Elimination Kinetics of Trimethyl Orthovalerate and Trimethyl Orthochloroacetate. *J. Phys. Chem. A* **2010**, *114*, 4203–4209. [CrossRef] [PubMed]
27. Lezama, J.; Márquez, E.; Mora, J.R.; Córdova, T.; Chuchani, G.; Cordova-Sintjago, T. Theoretical calculations on the mechanisms of the gas phase elimination kinetics of chlorocyclohexane, 3-chlorocyclohexene and 4-chlorocyclohexene. *J. Mol. Struct. THEOCHEM* **2009**, *916*, 17–22. [CrossRef]
28. Luiggi, M.; Mora, J.R.; Loroño, M.; Márquez, E.; Lezama, J.; Córdova, T.; Chuchani, G. Theoretical calculations on the gas-phase thermal decomposition kinetics of selected thiomethyl chloroalkanes: A new insight of the mechanism. *Comput. Theor. Chem.* **2014**, *1027*, 165–172. [CrossRef]
29. Farhadi, A.; Noei, J.; Aliyari, R.H.; Albakhtiyari, M.; Takassi, M.A. Experimental and theoretical study on a one-pot, three-component route to 3,4-dihydropyrimidin-2(1H)-ones/thiones TiCl3OTf-[bmim]Cl. *Res. Chem. Intermed.* **2016**, *42*, 1401–1409. [CrossRef]
30. Lu, N.; Chen, D.; Zhang, G.; Liu, Q. Theoretical investigation on enantioselective Biginelli reaction catalyzed by natural tartaric acid. *Int. J. Quantum Chem.* **2011**, *111*, 2031–2038. [CrossRef]
31. Glendening, E.D.; Landis, C.R.; Weinhold, F. NBO 6.0: Natural bond orbital analysis program. *J. Comput. Chem.* **2013**, *34*, 1429–1437. [CrossRef]
32. Stadler, A.; Kappe, C.O. Automated Library Generation Using Sequential Microwave-Assisted Chemistry. Application toward the Biginelli Multicomponent Condensation. *J. Comb. Chem.* **2001**, *3*, 624–630. [CrossRef]
33. Manhas, M.S.; Ganguly, S.N.; Mukherjee, S.; Jain, A.K.; Bose, A.K. Microwave-Initiated Reactions: Pechmann Coumarin Synthesis, Biginelli Reaction, and Acylation. *Tetrahedron Lett.* **2006**, *37*, 2423–2425. [CrossRef]
34. Wan, J.-P.; Lin, Y.; Hu, K.; Liu, Y. Secondary amine-initiated three-component synthesis of 3,4-dihydropyrimidinones and thiones involving alkynes, aldehydes and thiourea/urea. *Beilstein J. Org. Chem.* **2014**, *10*, 287–292. [CrossRef]



© 2019 by the authors. Licensee MDPI, Basel, Switzerland. This article is an open access article distributed under the terms and conditions of the Creative Commons Attribution (CC BY) license (http://creativecommons.org/licenses/by/4.0/).